




---

This is the **accepted version** of the article:

Muñoz Enano, Jonathan; Vélez Rasero, Paris; Martín, Ferran. «Signal balancing in unbalanced transmission lines». *IEEE Transactions on Microwave Theory and Techniques*, Vol. 67, issue 8 (Aug. 2019), p. 3339-3349. DOI 10.1109/TMTT.2019.2922598

---

This version is available at <https://ddd.uab.cat/record/221401>

under the terms of the  <sup>IN</sup> COPYRIGHT license

# Signal Balancing in Unbalanced Transmission Lines

Jonathan Muñoz-Enano, *Member IEEE*, Paris Véléz, *Member IEEE*, and Ferran Martín, *Fellow IEEE*

**Abstract**— Balanced lines operating as transmission line interconnects are subjected to differential-mode to common-mode conversion (and vice versa) in situations where symmetry imbalances (e.g., caused by line bends) are unavoidable. In this paper, a technique to compensate for such symmetry imbalances, providing pure differential-mode signals at the differential output port of the line, is presented. Such technique uses a rat-race balun (to generate the differential-mode signal) with the isolated port conveniently loaded, and it is based on the modification of the characteristic impedance of one of the unbalanced lines. A detailed analysis that justifies this compensation technique (valid for any arbitrary four-port network) and provides the design equations is presented. The approach is validated through simulation and experiment, by demonstrating that common-mode signals are not transmitted to the differential output port of a bended (i.e., unbalanced) line pair.

**Index Terms**— Balanced lines, Common-mode, Differential-mode, Microstrip, Rat-race coupler.

## I. INTRODUCTION

DIFFERENTIAL-MODE signals exhibit high immunity to electromagnetic interference (EMI), noise and crosstalk, as compared to single-ended signals. For that reason, differential (or balanced) transmission lines and circuits are becoming increasingly more common in modern communication systems [1]-[3]. A well known phenomenon in balanced lines and circuits is mode conversion, caused by imperfect symmetry. This may occur, for instance, in balanced transmission line interconnects, where line bending is sometimes necessary in order to accommodate such lines within the considered differential system avoiding an extra area. Thus, the generation of common-mode noise in imperfectly balanced lines due to cross-mode conversion (from the differential-mode signals) is almost unavoidable. Such common-mode noise, in turn, may produce radiation and EMI problems in the differential system, and may cause the degradation of the differential signals.

Many efforts have been dedicated in the last years to the design of common-mode filters. Such filters, typically (but not exclusively) based on defected ground structures (DGS) [4]-[22], must inhibit the propagation of common-mode signals in the balanced line, and simultaneously preserve the integrity of the differential signals. In high-speed differential-mode interconnects, wideband signals are

involved, and this justifies the intensive activity towards the design of high-rejection level and broad-band common-mode filters. However, in applications where narrow-band differential-mode signals are involved, the need to reject the common mode over a wide band is not a strong requirement.

In this paper, an alternative approach to common-mode filters, to suppress the common mode in imperfectly balanced lines is proposed. The technique uses a rat-race balun to generate the differential mode signal from a single-ended signal, and the load termination at the isolated port of the rat race is a design parameter. With the convenient load, and an adequate adjustment of the characteristic impedance in one of the lines of the imperfectly balanced differential line pair, it is found that the common-mode at the output differential port is efficiently suppressed. Therefore, the proposed structure, including the rat-race balun plus the (deliberately) modified unbalanced line, corrects the effects of symmetry imbalances in the line pair through mode conversion compensation. As long as a rat-race is involved in the proposed technique, system functionality is limited to narrow-band signals operating in the vicinity of the design frequency of the rat-race coupler. The device can be considered to be a single-ended to differential-mode converter, able to compensate for symmetry imbalances.

The paper is organized as follows: Section II presents the structure under study and an exhaustive analysis focused on obtaining the conditions for signal balancing in arbitrary four-port networks. In section III, such analysis is particularized to the case of a pair of unbalanced lines. It is found that by terminating the isolated port of the rat-race coupler with an open or shorted stub of adequate length and by adjusting the characteristic impedance of one of the lines, it is possible to generate balanced signals at the output differential port of the line pair. The validation of the reported signal balancing approach is carried out in Section IV, by considering circuit, electromagnetic simulations and experiments. Section V is dedicated to a discussion related to return losses, unavoidable in the proposed balancing strategy. Finally, the main conclusions of the work are highlighted in Section VI.

## II. THE BALANCING STRUCTURE AND ANALYSIS

The structure under study consists of an arbitrary (potentially unbalanced) four-port network preceded by a rat-race balun with the isolated port ( $\Sigma$ -port) terminated with a load (a design parameter), characterized by a reflection coefficient,  $\rho$  (see Fig. 1). If the four-port network exhibits perfect symmetry with regard to the indicated axial plane (i.e., it is balanced), pure differential-mode signals are generated at the output composite port ( $A'-B'$ ), regardless of the value of  $\rho$ . Note that the input port of the whole structure is the  $\Delta$ -port of the coupler, thereby generating out-of-phase signals at ports 3 and 4 of

---

Manuscript received Month DD, YYYY; revised Month DD, YYYY; accepted Month DD, YYYY. This work was supported by MINECO-Spain (project TEC2016-75650-R), by *Generalitat de Catalunya* (project 2017SGR-1159), by *Institució Catalana de Recerca i Estudis Avançats* (who awarded Ferran Martín), and by FEDER funds. J. Muñoz-Enano acknowledges *Secretaria d'Universitats i Recerca* (Gen. Cat.) and *European Social Fund* for the FI grant. Paris Véléz acknowledges the Juan de la Cierva Program for supporting him through Project IJCI-2017-31339.

J. Muñoz-Enano, P. Véléz, and F. Martín are with GEMMA/CIMITEC, Departament d'Enginyeria Electrònica, Universitat Autònoma de Barcelona, 08193 Bellaterra, Spain. E-mail: [Ferran.Martin@uab.es](mailto:Ferran.Martin@uab.es).

the coupler, which are transmitted through the balanced four-port network as a pure differential-mode signal.

By truncating symmetry, mode conversion in the unbalanced four-port network arises, and, in general, common-mode signal components at the output composite port A'-B' of the network are expected. However, by properly choosing the load termination of the isolated port of the coupler (i.e.,  $\rho$ ), it is possible to compensate for the effects of mode conversion in the unbalanced network, and thus suppress the common mode at the composite port A'-B' (at least in cases of special interest, to be considered later). The net effect is signal balancing in the (otherwise) unbalanced four-port network.

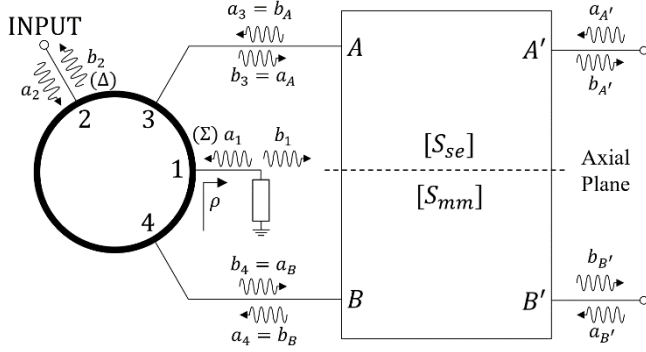


Fig. 1. Arbitrary four-port network preceded by a rat-race coupler balun with the isolated port terminated with a load impedance. By adequately choosing the impedance of such load, signal balancing (i.e., a pure differential-mode signal) can be generated at the output composite port.

To demonstrate the potential of the structure to generate (ideally) pure differential-mode signals in unbalanced networks, it is necessary to calculate the transmission coefficient between the input port (port 2 of the coupler) and the output ports (ports A' and B' of the unbalanced four-port network). For that purpose, ports A' and B' must be terminated with matched loads, and the corresponding normalized amplitudes of the voltage waves at those ports ( $b_{A'}$  and  $b_{B'}$ ) must be expressed as a function of the normalized amplitude of the voltage wave impinging at the input port (port 2 of the coupler),  $a_2$ . The first step is to write  $b_{A'}$  and  $b_{B'}$  in terms of the impinging waves at ports A and B of the four-port network, that is,

$$b_{A'} = S_{A'A}a_A + S_{A'B}a_B = S_{A'A}b_3 + S_{A'B}b_4 \quad (1a)$$

$$b_{B'} = S_{B'A}a_A + S_{B'B}a_B = S_{B'A}b_3 + S_{B'B}b_4 \quad (1b)$$

where a subset of elements of the single-ended S-parameter matrix of the four-port network, given by

$$\mathbf{S}_{se} = \begin{pmatrix} S_{AA} & S_{AA'} & S_{AB} & S_{AB'} \\ S_{A'A} & S_{A'A'} & S_{A'B} & S_{A'B'} \\ S_{BA} & S_{BA'} & S_{BB} & S_{BB'} \\ S_{B'A} & S_{B'A'} & S_{B'B} & S_{B'B'} \end{pmatrix}, \quad (2)$$

has been used.

According to the well-known S-parameter matrix of the rat-race coupler [23],  $b_3$  and  $b_4$  can be expressed as

$$b_3 = -\frac{j}{\sqrt{2}}(a_1 + a_2) = -\frac{j}{\sqrt{2}}(\rho b_1 + a_2) \quad (3a)$$

$$b_4 = -\frac{j}{\sqrt{2}}(a_1 - a_2) = -\frac{j}{\sqrt{2}}(\rho b_1 - a_2), \quad (3b)$$

and by introducing (3) in (1), the following expressions are obtained:

$$b_{A'} = -\frac{j}{\sqrt{2}}\{(S_{A'A} + S_{A'B})\rho b_1 + (S_{A'A} - S_{A'B})a_2\} \quad (4a)$$

$$b_{B'} = -\frac{j}{\sqrt{2}}\{(S_{B'A} + S_{B'B})\rho b_1 + (S_{B'A} - S_{B'B})a_2\} \quad (4b)$$

On the other hand, the normalized amplitude of the voltage wave impinging at the load of port 1,  $b_1$ , can be expressed as

$$b_1 = -\frac{j}{\sqrt{2}}(a_3 + a_4) = -\frac{j}{\sqrt{2}}(b_A + b_B) \quad (5)$$

where  $b_A$  and  $b_B$  are given by

$$b_A = S_{AA}b_3 + S_{AB}b_4 \quad (6a)$$

$$b_B = S_{BA}b_3 + S_{BB}b_4 \quad (6b)$$

Introducing (3) in (6), and the resulting expression in (5), the following expression results:

$$b_1 = -\{S_{11}^{cc}\rho b_1 + S_{11}^{cd}a_2\} \quad (7)$$

where a pair of elements of the mixed-mode S-parameter matrix of the four-port network [2],[25],[26] are involved. Such matrix can be expressed in the following form

$$\mathbf{S}_{mm} = \begin{pmatrix} \mathbf{S}^{dd} & \mathbf{S}^{dc} \\ \mathbf{S}^{cd} & \mathbf{S}^{cc} \end{pmatrix} = \begin{pmatrix} S_{11}^{dd} & S_{12}^{dd} & S_{11}^{dc} & S_{12}^{dc} \\ S_{21}^{dd} & S_{22}^{dd} & S_{21}^{dc} & S_{22}^{dc} \\ S_{11}^{cd} & S_{12}^{cd} & S_{11}^{cc} & S_{12}^{cc} \\ S_{21}^{cd} & S_{22}^{cd} & S_{21}^{cc} & S_{22}^{cc} \end{pmatrix} \quad (8)$$

with [2]

$$\mathbf{S}^{dd} = \frac{1}{2} \begin{pmatrix} S_{AA} - S_{AB} - S_{BA} + S_{BB} & S_{A'A} - S_{A'B} - S_{B'A} + S_{B'B} \\ S_{A'A} - S_{A'B} - S_{B'A} + S_{B'B} & S_{A'A} - S_{A'B} - S_{B'A} + S_{B'B} \end{pmatrix} \quad (9a)$$

$$\mathbf{S}^{cc} = \frac{1}{2} \begin{pmatrix} S_{AA} + S_{AB} + S_{BA} + S_{BB} & S_{A'A} + S_{A'B} + S_{B'A} + S_{B'B} \\ S_{A'A} + S_{A'B} + S_{B'A} + S_{B'B} & S_{A'A} + S_{A'B} + S_{B'A} + S_{B'B} \end{pmatrix} \quad (9b)$$

$$\mathbf{S}^{dc} = \frac{1}{2} \begin{pmatrix} S_{AA} + S_{AB} - S_{BA} - S_{BB} & S_{A'A} + S_{A'B} - S_{B'A} - S_{B'B} \\ S_{A'A} + S_{A'B} - S_{B'A} - S_{B'B} & S_{A'A} + S_{A'B} - S_{B'A} - S_{B'B} \end{pmatrix} \quad (9c)$$

$$\mathbf{S}^{cd} = \frac{1}{2} \begin{pmatrix} S_{AA} - S_{AB} + S_{BA} - S_{BB} & S_{A'A} - S_{A'B} + S_{B'A} - S_{B'B} \\ S_{A'A} - S_{A'B} + S_{B'A} - S_{B'B} & S_{A'A} - S_{A'B} + S_{B'A} - S_{B'B} \end{pmatrix} \quad (9d)$$

By isolating  $b_1$  from (7), the following result is obtained

$$b_1 = -\frac{S_{11}^{cd}a_2}{1+S_{11}^{cc}\rho}, \quad (10)$$

and, finally, by introducing (10) in (4), the transmission coefficients between port 2 of the coupler (the input port) and ports A' and B' of the four-port network (the output ports) are found to be

$$S_{A'2} = \left. \frac{b_{A'}}{a_2} \right|_{a_{A'}=a_{B'}=0} = -\frac{j}{\sqrt{2}} \left\{ \frac{S_{A'A} - S_{A'B} + (S_{A'A} - S_{A'B})S_{11}^{cc}\rho - (S_{A'A} + S_{A'B})S_{11}^{cd}\rho}{1+S_{11}^{cc}\rho} \right\} \quad (11a)$$

$$S_{B'2} = \left. \frac{b_{B'}}{a_2} \right|_{a_{A'}=a_{B'}=0} = -\frac{j}{\sqrt{2}} \left\{ \frac{S_{B'A} - S_{B'B} + (S_{B'A} - S_{B'B})S_{11}^{cc}\rho - (S_{B'A} + S_{B'B})S_{11}^{cd}\rho}{1+S_{11}^{cc}\rho} \right\} \quad (11b)$$

Note that if the four-port network is balanced, the elements of the cross-mode matrices,  $\mathbf{S}^{cd}$  and  $\mathbf{S}^{dc}$ , are null. Moreover,  $S_{A'B} = S_{B'A}$  and  $S_{A'A} = S_{B'B}$  in a balanced network. Therefore, according to (11),  $S_{A'2} = -S_{B'2}$ , and the signals generated at ports A' and B' are out-of-phase. Hence, a pure differential-mode signal is generated at the composite port

A'-B' of a balanced network, regardless of the value  $\rho$  (as anticipated before).

The reflection coefficient at the input port of the structure,  $S_{22}$ , can be obtained following a similar procedure (which is not repeated). The result is

$$S_{22} = \frac{b_2}{a_2} \Big|_{a_{A'}=a_{B'}=0} = \frac{\rho S_{11}^{dc} S_{11}^{cd}}{1 + S_{11}^{cc} \rho} - S_{11}^{dd} \quad (12)$$

and it coincides with  $S_{11}^{dd}$  (except the sign) in a balanced network. It is also interesting to mention that for a balanced network, the normalized amplitude of the wave voltage impinging at the load of the isolated port of the coupler (port 1) is null, as derived from (10). Therefore, no energy is dissipated in the system for lossless balanced networks, regardless of the load present at port 1 of the coupler.

Let us now consider that the four-port network is an arbitrary (potentially unbalanced) network, and let us force  $S_{A'2} = -S_{B'2}$ , in order to obtain a pure differential signal at the composite port A'-B'. This balancing condition is satisfied if the reflection coefficient of the load at port 1 is

$$\rho = \frac{S_{21}^{cd}}{S_{11}^{cd} S_{21}^{cc} - S_{11}^{cc} S_{21}^{cd}} \quad (13)$$

From (13), it is not apparent that a solution with a passive load (i.e., with  $|\rho| \leq 1$ ) always exists. Nevertheless, this analysis opens the path to signal balancing in unbalanced structures, as it will be corroborated in a specific four-port network of practical interest, to be discussed in the next section. Although balancing in such network is not always possible (as it will be demonstrated), such imbalance is restricted to specific cases of limited interest.

### III. BALANCING UNBALANCED TRANSMISSION LINES

Let us now consider a specific four-port network consisting of a pair of uncoupled lines. This case is of special interest since line bending, unavoidable in many situations involving differential line pairs, generates mode conversion. Indeed, a bended line pair exhibits different electrical length, or phase shift, in the individual lines, and for that reason pure differential signals cannot be transmitted along the structure. Therefore, our aim is to compensate for the effects of the different phase of the lines by terminating port 1 of the coupler according to (13).

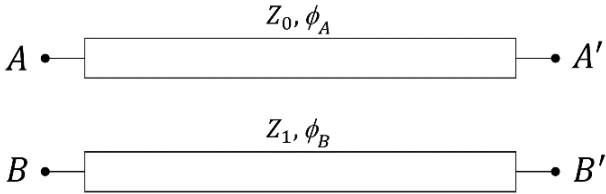


Fig. 2. Schematic of the unbalanced transmission line pair under study.

Let us designate as line A the one between ports A and A', and as line B the one between ports B and B'. The corresponding electrical lengths at the operating frequency are called  $\phi_A$  and  $\phi_B$ , respectively. In an uncoupled balanced line pair, the characteristic impedance of the individual lines is typically the reference impedance of the ports,  $Z_0$ . Nevertheless, in the present study, the characteristic impedance of line B, designated as  $Z_1$ , is considered as a design parameter. This offers higher design flexibility, and, indeed, it is not possible to achieve signal

balancing at the output composite port of a pair of lines with unequal phase shift if  $Z_1 = Z_0$ , as it will be shown. Hence, considering  $Z_1$  as a design parameter is a need for our purposes (signal balancing in a bended line pair). Thus, the four-port network to be studied is the one depicted in Fig. 2.

Using (9), and taking into account that the considered lines are uncoupled (i.e., any single-ended S-parameter involving sub-indexes referred to ports of both lines are null), expression (13) can be written as

$$\rho = \frac{S_{A'A} - S_{B'B}}{S_{AA} S_{B'B} - S_{BB} S_{A'A}} \quad (14)$$

where  $S_{AA} = 0$  by virtue of the matching condition for line A (i.e.,  $Z_A = Z_0$ ), and

$$S_{A'A} = \frac{1}{\cos \phi_A + j \sin \phi_A} \quad (15a)$$

$$S_{B'B} = \frac{2}{2 \cos \phi_B + j \left( \frac{Z_1 + Z_0}{Z_0} \right) \sin \phi_B} \quad (15b)$$

$$S_{BB} = \frac{j \left( \frac{Z_1 - Z_0}{Z_0} \right) \sin \phi_B}{2 \cos \phi_B + j \left( \frac{Z_1 + Z_0}{Z_0} \right) \sin \phi_B} \quad (15c)$$

Separating the real and the imaginary parts of  $\rho$ , one obtains

$$Re\{\rho\} = \frac{2 \sin \phi_A - \left( \frac{Z_1 + Z_0}{Z_0} \right) \sin \phi_B}{\left( \frac{Z_1 - Z_0}{Z_0} \right) \sin \phi_B} \quad (16a)$$

$$Im\{\rho\} = -\frac{2(\cos \phi_A - \cos \phi_B)}{\left( \frac{Z_1 - Z_0}{Z_0} \right) \sin \phi_B} \quad (16b)$$

Note that if  $\rho$  is a real number and it satisfies  $|\rho| \leq 1$ , the load is a pure resistance (or either an open or a short circuit for the extreme cases of  $\rho = \pm 1$ ). However, inspection of (16) reveals that  $Im\{\rho\}$  can only be null under very specific conditions ( $\cos \phi_A = \cos \phi_B$ ), which are not of interest, as long as line bending in a line pair produces imbalances in the phase of the lines. In general,  $\rho$  is a complex number, but it should satisfy  $|\rho| \leq 1$  for the validity of the balancing approach by means of port termination with a passive load. Thus, let us calculate the modulus of  $\rho$ , and let us force it to satisfy  $|\rho| \leq 1$ . After some tedious calculation,  $|\rho|$  can be expressed as

$$|\rho| = \frac{1}{\left| \left( \frac{Z_1 - Z_0}{Z_0} \right) \sin \phi_B \right|} \sqrt{\left( \frac{Z_1 - Z_0}{Z_0} \right)^2 \sin^2 \phi_B + 4R} \quad (17)$$

where the residual part of the root,  $R$ , is given by

$$R = 2 - \cos(\phi_A - \phi_B) [T + 1] + \cos(\phi_A + \phi_B) [T - 1] \quad (18)$$

and

$$T = \frac{1}{2} \left( \frac{Z_1}{Z_0} + \frac{Z_0}{Z_1} \right) \quad (19)$$

From (17), it is apparent that a passive solution for the load of the isolated port of the coupler exists as long as  $R \leq 0$  (corresponding to  $|\rho| \leq 1$ ). Thus, from the elements characterizing the network (i.e.,  $\phi_A$ ,  $\phi_B$ , and  $Z_1$ ), we can evaluate  $R$  and, from the resulting value, we can discern if signal balancing with a passive load is possible or not.

### A. Impedance Imbalance

Although considering identical phases for the lines A and B is not of practical interest (for the reasons explained before), in this case ( $\phi_A = \phi_B = \phi$ ),  $R$  is found to be

$$R = \frac{(Z_1 - Z_0)^2}{2Z_1 Z_0} (\cos 2\phi - 1) \leq 0 \quad (20)$$

and the solution for the port termination (a passive load) is, in general, a pure resistance (since  $\text{Im}\{\rho\} = 0$  for  $\phi_A = \phi_B$ ). There are, however, two extreme situations, providing  $R = 0$ , that require special attention. One corresponds to the case of identical line impedances matched to the ports ( $Z_1 = Z_0$ ). In this case, there is not a mathematical solution for  $\rho$ , according to (16). However, since  $Z_1 = Z_0$  and  $\phi_A = \phi_B$ , the four-port network is perfectly balanced, and any signal at the composite port A'-B' is a pure differential signal, regardless of the load present at port 1 of the coupler, as discussed in the previous section. The second case corresponds to line lengths of half-wavelength, or multiple of it (i.e.,  $\phi = n\pi$ , with  $n = 0, 1, 2, 3, \dots$ ). A mathematical solution of (16) does not exist either. For such line lengths, the matched terminations of ports A' and B' are translated to ports 3 and 4, respectively, of the coupler, regardless of the characteristic impedance of the lines, and a pure differential signal is also generated at the composite port A'-B'. The influence of any load present at port 1 of the coupler on signal balancing is also null in this case.

Interestingly, for  $\phi_A = \phi_B = \phi$  with  $\phi \neq n\pi$  and  $Z_1 \neq Z_0$ , solution of (16) gives

$$\rho = -\frac{Z_1 - Z_0}{Z_1 + Z_0} \quad (21)$$

corresponding to a resistive load (as anticipated before) given by

$$Z_\rho = \frac{Z_0^2}{Z_1} \quad (22)$$

and such resistance does not depend on the phase of the lines. To summarize, for a pair of uncoupled lines with identical electrical length but different characteristic impedance, terminating the isolated port of the coupler (port 1) with a resistance given by (22), suffices to obtain a pure differential signal at the output composite port A'-B' (signal balancing). Moreover, for the particular case of half-wavelength line lengths (or multiples), signal balancing is achieved regardless of port 1 termination.

### B. Phase Imbalance

Let us now consider the general case of different electrical lengths ( $\phi_A \neq \phi_B$ ), such as occurs in bended differential line pairs. Inspection of (17) indicates that if  $Z_1 = Z_0$ , then  $|\rho| = \infty$ , since  $R = 2[1 - \cos(\phi_A - \phi_B)] > 0$ . Therefore, signal balancing cannot be achieved unless  $Z_1 \neq Z_0$ . In other words, in order to achieve a pure differential-mode signal at the output composite port of a pair of bended lines, it is necessary to further imbalance the structure by varying the characteristic impedance of one of the lines. In this case,  $\rho$  is, in general, a complex number with a modulus depending on the phases of the lines  $\phi_A$  and  $\phi_B$ , as well as on the ratio of line impedances  $Z_1/Z_0$ .

In general  $\phi_A$  and  $\phi_B$  are not design parameters, but the ratio  $Z_1/Z_0$  (or normalized impedance of line B,  $\bar{Z}_1$ ) can be properly adjusted in order to satisfy certain requirements

(i.e., it can be considered as a design parameter). Particularly, a normalized impedance providing exactly  $|\rho| = 1$  (or  $R = 0$ ), if it exists, is very convenient, since in this case signal balancing can be achieved by means of a pure reactive termination at port 1 of the coupler (in practice implementable by means of an open or shorted stub). Thus, let us force  $R = 0$ . From (18), the following condition is obtained

$$T = \csc \phi_A \cdot \csc \phi_B - \cot \phi_A \cdot \cot \phi_B \quad (23)$$

According to (19),  $T \geq 1$  for any resistive impedance  $Z_1$ . Therefore, the solution of (23) should provide a value of  $T$  satisfying the previous requirement in order to achieve signal balancing with a pure reactive termination of port 1 of the coupler. The dependence of  $T$  with  $\phi_A$  and  $\phi_B$  is depicted in Fig. 3, where the allowed regions ( $T \geq 1$ ) are visible. For a given pair of phases  $\phi_A$  and  $\phi_B$  (corresponding to a certain position in the  $\phi_A$ - $\phi_B$  plane) belonging to the allowed regions, by choosing the value of  $T$  given by (23), the solution to achieve signal balancing is a pure reactive load ( $|\rho| = 1$ ). If we choose  $T$  different from this value and such value gives  $R < 0$ , then the solution is a complex load.

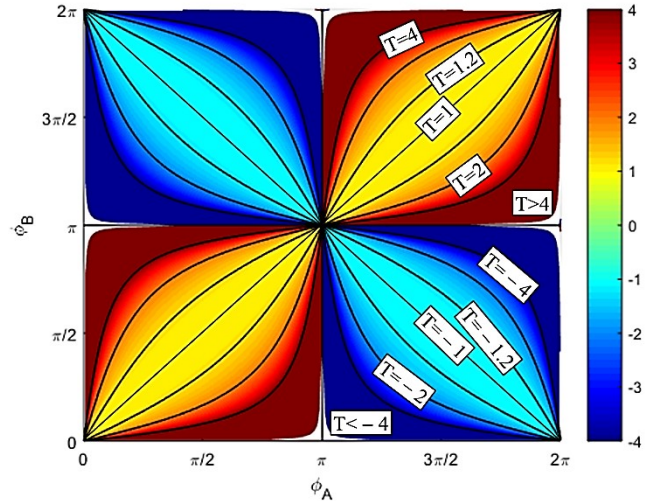


Fig. 3. Dependence of  $T$  with  $\phi_A$  and  $\phi_B$ . The allowed regions ( $T \geq 1$ ) are given by those combinations of  $\phi_A$  and  $\phi_B$  satisfying  $n\pi < \phi_A < (n+1)\pi$  and  $m\pi < \phi_B < (m+1)\pi$ , with  $n, m = 0, 1, 2, 3, \dots$  and  $n + m$  an even number.

It is interesting to mention that there are not mathematical solutions of (23) for  $\phi_A = n\pi$  or  $\phi_B = n\pi$ . In this case,  $T = \infty$  (and  $\bar{Z}_1 = \infty$  or 0), unless  $\phi_A = \phi_B = n\pi$  (a particular situation analyzed before). It can be also seen that if  $\phi_A = \phi_B$ , then  $T = 1$ , corresponding to  $\bar{Z}_1 = 1$  (or  $Z_1 = Z_0$ ), as inferred from (20) if  $\phi_A = \phi_B \neq n\pi$ . In most practical cases of bended line pairs, the phases of the lines are not expected to differ so much ( $\phi_A \approx \phi_B$ ). In other words, the phase combinations are expected to lie close to the diagonal line in the  $\phi_A$ - $\phi_B$  plane (with  $T = 1$ ), where solutions of (23) with moderate value for  $T$  do exist, thereby providing moderate values of  $\bar{Z}_1$ , as well (this is a strong practical requirement as far as the impedance of line B cannot take extreme values).

From (19), the pair of solutions for  $\bar{Z}_1$  are

$$\bar{Z}_1 = T(1 \pm \sqrt{1 - T^{-2}}) \quad (24)$$

and these solutions verify that their product is 1. By introducing (23) in (24), and after some simple algebra, it has been found that the pair of solutions for the normalized

impedance of line B can be expressed in the following compact form

$$\bar{Z}_1 \equiv \frac{Z_1}{Z_0} = \frac{(1 \pm \cos \phi_A)(1 \mp \cos \phi_B)}{\sin \phi_A \sin \phi_B} \quad (25)$$

Using (25), the following terms, necessary for the evaluation of  $\rho$  (see expression 16), are obtained:

$$\frac{Z_1}{Z_0} + \frac{Z_0}{Z_1} = 2T = \frac{2\{1 - \cos \phi_A \cos \phi_B\}}{\sin \phi_A \sin \phi_B} \quad (26a)$$

$$\frac{Z_1}{Z_0} - \frac{Z_0}{Z_1} = \frac{2\{1 - \cos \phi_A \cos \phi_B\}}{\sin \phi_A \sin \phi_B} - \frac{2 \sin \phi_A \sin \phi_B}{(1 \pm \cos \phi_A)(1 \mp \cos \phi_B)} \quad (26b)$$

By introducing such terms in (16), the two solutions of  $\rho$  are found to be

$$\rho = \mp \cos \phi_A \mp j \sin \phi_A = \mp e^{j\phi_A} \quad (27)$$

and  $|\rho| = 1$ , as expected. Finally, once the value of  $\rho$  is known, the pair of impedances (purely reactive) that must be used to terminate port 1 of the coupler for signal balancing are found to be

$$Z_\rho = Z_0 \frac{1+\rho}{1-\rho} = Z_0 \frac{\mp j \sin \phi_A}{1 \pm \cos \phi_A} \quad (28)$$

Note that in (28) the upper/lower sign of the solution corresponds to the normalized impedance of line B given by the upper/lower sign in (25). The (-) and (+) solutions of (27) correspond to the input reflection coefficients of a short-ended and open-ended stub, respectively, with electrical length given by  $\phi_{stub} = n\pi - \phi_A/2$  ( $n$  being an integer number such that  $\phi_{stub} > 0$ ), see Fig. 4. This is apparent as far as (27) can be expressed as

$$\rho = \mp e^{-2j\left(n\pi - \frac{\phi_A}{2}\right)} \quad (29)$$

which is the reflection coefficient of a stub with the above-cited electrical length, terminated with an open circuit (+ solution) or with a short circuit (- solution), as it is well known [23]. To further confirm this assertion, the input impedance of the open- and short-ended stubs of Fig. 4 can be written as [23]

$$Z_{o.c} = -jZ_0 \cot\left(n\pi - \frac{\phi_A}{2}\right) = jZ_0 \cot\left(\frac{\phi_A}{2}\right) = Z_0 \frac{j \sin \phi_A}{1 - \cos \phi_A} \quad (30a)$$

$$Z_{s.c} = jZ_0 \tan\left(n\pi - \frac{\phi_A}{2}\right) = -jZ_0 \tan\left(\frac{\phi_A}{2}\right) = -Z_0 \frac{j \sin \phi_A}{1 + \cos \phi_A} \quad (30b)$$

and these expressions coincide with (28).

Thus, from the previous analysis it follows that if two uncoupled lines exhibit different electrical length, signal balancing at the output composite port (i.e., the generation of a pure differential signal at that port) is straightforward. It is simply achieved by deliberately varying the characteristic impedance of one of the lines (according to 25) and by terminating the isolated port of the rat-race balun (used to feed the lines) by means of a stub with the characteristics shown in Fig. 4. Note that the short-ended stub of Fig. 4(b) can be alternatively replaced with an open-ended stub with length  $(n+1/2)\pi - \phi_A/2$ , hence avoiding the use of vias to terminate the stub. Figure 4 considers the two balancing solutions with a purely reactive load at the isolated port of the rat-race coupler. This is the case of foremost interest as far as the implementation of the reactive load is carried out by means of open or short-ended

stubs. For clear understanding, and for design purposes, Fig. 4 depicts the values of the electrical length and characteristic impedance for the stub and line B for the two balancing solutions.

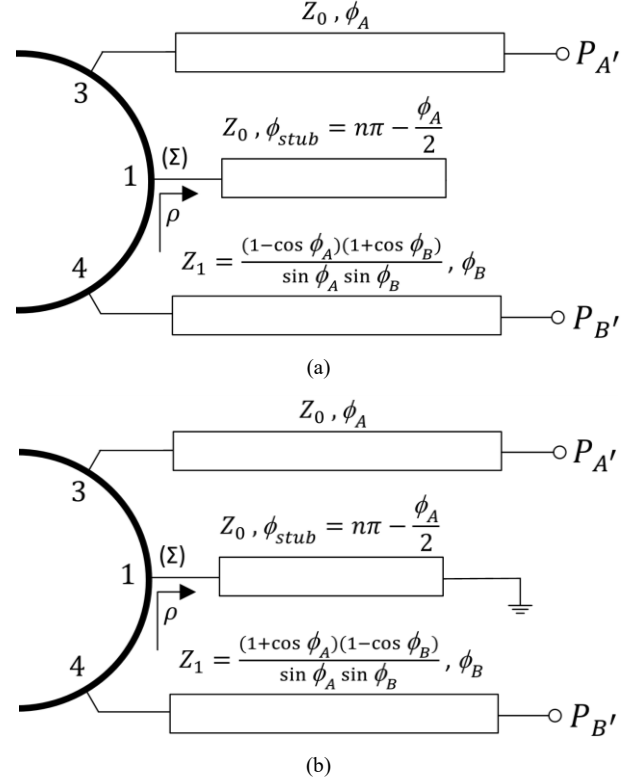


Fig. 4. Stubs providing the reflection coefficients given by expressions (27) or (29), necessary at the isolated port of the balun in order to achieve signal balancing. (a) (+) solution; (b) (-) solution. The corresponding solution for  $Z_1$  is also indicated.

#### IV. VALIDATION

Validation of the previous analysis is first carried out through circuit simulation (using *Keysight ADS*) by considering ideal lines and coupler, and then through electromagnetic simulation (using *Keysight Momentum*) and experiment.

##### A. Circuit Simulation

To verify the validity of the previous analysis we have first considered ideal lossless components under different cases, pointed out in the previous section. Let us first consider identical phases of both lines ( $\phi_A = \phi_B = \phi$ ), with  $\phi \neq n\pi$  and  $Z_1 \neq Z_0$ . Let us set the phase of both lines to  $\phi = \pi/2$  at  $f_0 = 2$  GHz, and the characteristic impedance of line B to  $Z_1 = \sqrt{2}Z_0$ . According to (22), the required termination of port 1 of the coupler in order to achieve signal balancing at the output composite port should be  $Z_\rho = Z_0/\sqrt{2}$ . This gives  $Z_\rho = 35.35\Omega$  for  $Z_0 = 50\Omega$ , the usual reference impedance of the ports. This case has been simulated by the circuit simulator of *Keysight ADS* and it is verified that  $S_{A'2} = -S_{B'2}$ , corresponding to perfect signal balancing. Actually, signal balancing should be achieved regardless of the phase of the lines,  $\phi$ , as far as  $Z_\rho$  does not depend on  $\phi$ . This is verified in Fig. 5, where  $S_{A'2}$  and  $S_{B'2}$  obtained for different values of  $\phi$  reveal that  $S_{A'2} = -S_{B'2}$  at  $f_0$  (the reflection from the ports is also included in the figure).



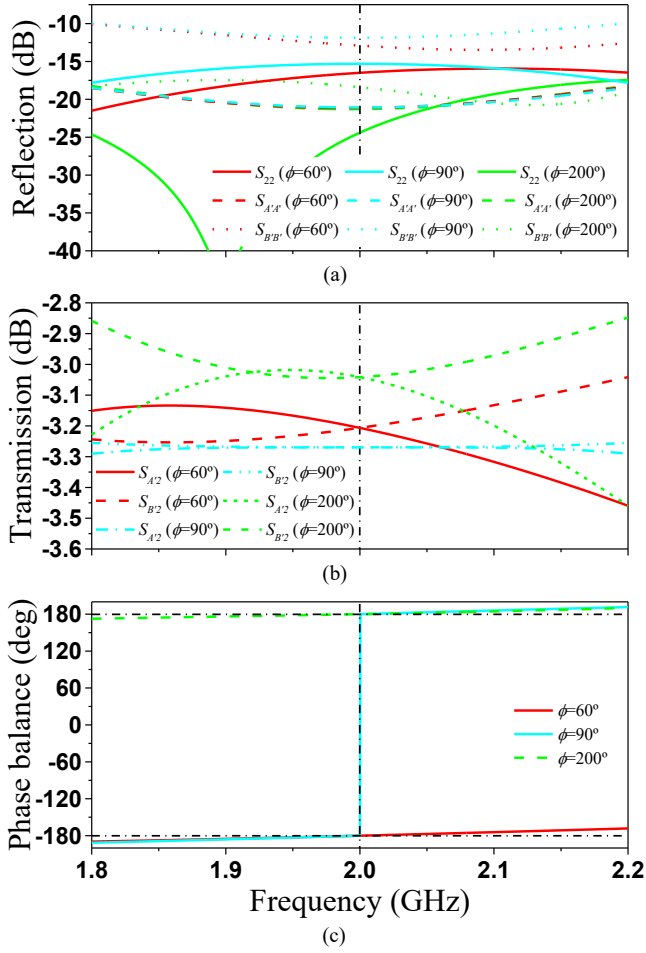


Fig. 5. S-parameters by considering signal balancing with resistive load (impedance imbalance). (a) Magnitude of the reflection from the ports; (b) magnitude of  $S_{A12}$  and  $S_{B2}$ ; (c) phase balance at the output ports.

Let us now consider signal balancing in a pair of lines with different electrical length ( $\phi_A \neq \phi_B$ ) by means of a pure reactive load. The phases have been set to  $\phi_A = 450^\circ$  and  $\phi_B = 480^\circ$  ( $f_0 = 2$  GHz). From these phase values and  $Z_0 = 50 \Omega$ , the two solutions of (25) for the characteristic impedance of line B are found to be  $Z_{1,u} = 86.6 \Omega$  and  $Z_{1,l} = 28.86 \Omega$ , where the additional sub-index ( $u$  or  $l$ ) indicate the solution corresponding to the upper ( $u$ ) or lower ( $l$ ) signs in (25). For  $Z_{1,u} = 86.6 \Omega$ , the electrical length of the  $50 \Omega$  short-ended stub that must be used to terminate port 1 of the coupler is  $135^\circ$ . For  $Z_{1,l} = 28.86 \Omega$ , the same electrical length is required, but the stub must be terminated by an open circuit. The two combinations of stub length and characteristic impedance of line B have been introduced in the circuit simulator of *Keysight ADS*, and it has been verified that  $S_{A12} = -S_{B2}$  at  $f_0$  [Fig. 6(b)]. Then, we have analyzed the tolerances of signal balancing against variations in both  $Z_1$  and  $\phi_{stub}$ . Figure 6 depicts  $S_{A12}$  and  $S_{B2}$  that results by slightly varying either  $Z_1$  or  $\phi_{stub}$  from the nominal values. It can be appreciated that perfect signal cancelation (balancing) exists when  $Z_1$  or  $\phi_{stub}$  are set to the nominal values, as expected. However, mode coupling progressively arises as  $Z_1$  or  $\phi_{stub}$  are perturbed (as indicated by the variation in the magnitude of  $S_{A12}$  and  $S_{B2}$  and in the phase balance).

To further illustrate the potential of the proposed signal balancing approach, let us consider a different combination of line phases, particularly,  $\phi_A = 200^\circ$  and  $\phi_B = 215^\circ$  (with

$f_0 = 2$  GHz). In this case, the two solutions for the characteristic impedance of line B are found to be  $Z_{1,u} = 89.41 \Omega$  and  $Z_{1,l} = 27.96 \Omega$ , whereas the electrical length of the short- or open-ended stub is found to be  $80^\circ$ . Figure 7 depicts the reflection from the input port, as well as the transmission coefficients to the output ports and phase balance at these ports. The results, again, reveal that signal balancing at the design frequency is achieved.

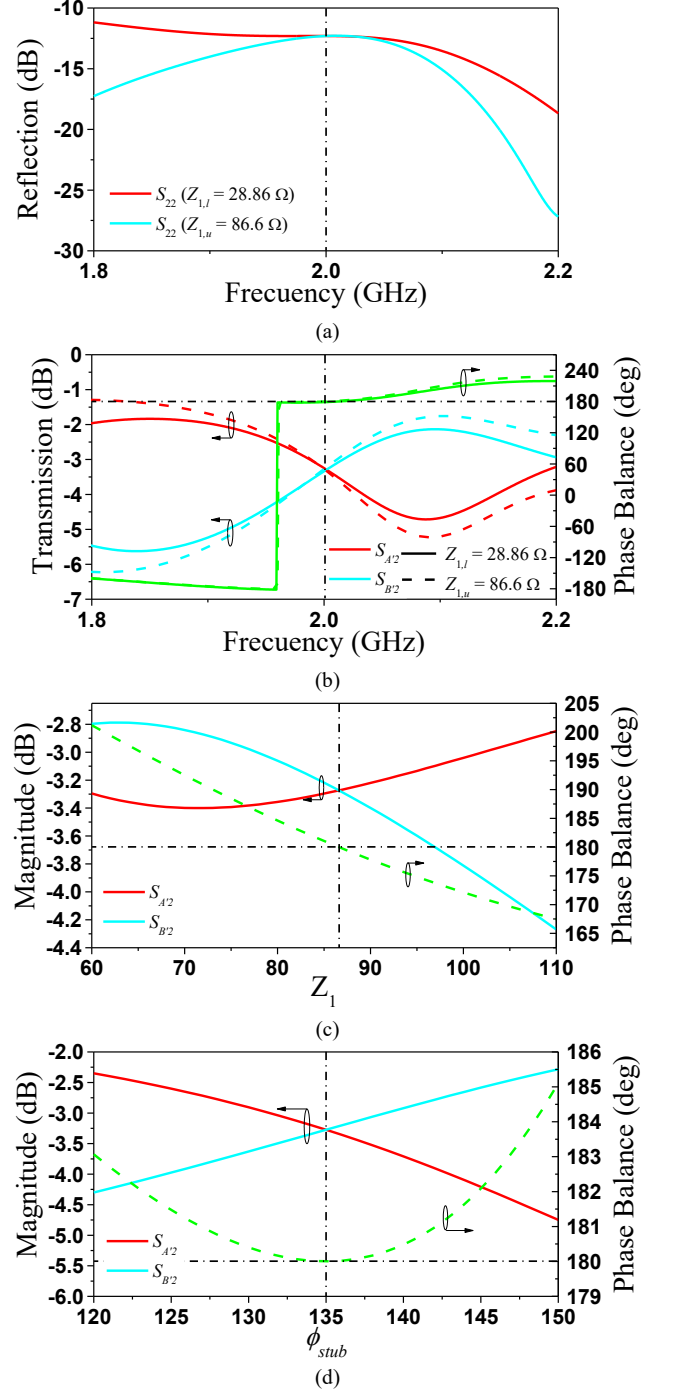


Fig. 6. Balancing with pure reactive load for a phase imbalance of the lines of  $\phi_A = 450^\circ$  and  $\phi_B = 480^\circ$ . (a) Reflection from the input port; (b) Magnitude of  $S_{A12}$  and  $S_{B2}$ , and phase balance at the output ports; (c) effects of perturbation of  $Z_1$  from the nominal value and (d) effects of perturbation of  $\phi_{stub}$  from the nominal value, for  $Z_{1,l} = 86.6 \Omega$  and short-ended stub case at the design frequency  $f_0 = 2$  GHz.

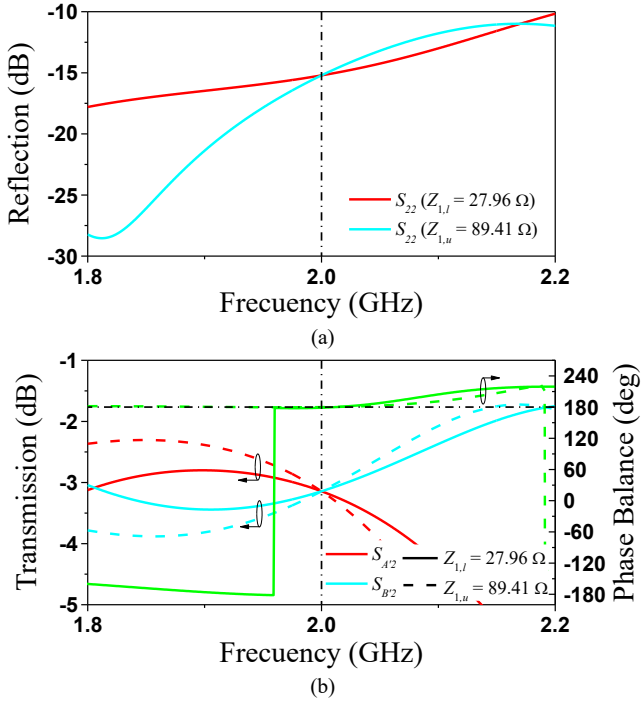


Fig. 7. Balancing with pure reactive load for a phase imbalance of the lines of  $\phi_A = 200^\circ$  and  $\phi_B = 215^\circ$ . (a) Reflection from the input port; (b) Magnitude of  $S_{A2}$  and  $S_{B2}$ , and phase balance at the output ports.

### B. Electromagnetic Simulation and Experiment

In this subsection, the cases considered before are validated through electromagnetic simulation (using *Keysight Momentum*) and measurement (using the *Agilent N5221A PNA* microwave network analyzer). For the unbalanced pair of lines with identical line phases but different characteristic impedances ( $\phi_A = \phi_B = \phi \neq n\pi$  and  $Z_1 \neq Z_0$ ), the photograph of the whole structure is depicted in Fig. 8 (corresponding to  $\phi = 200^\circ$  and  $Z_1 = \sqrt{2}Z_0 = 70.71 \Omega$ , with  $Z_0 = 50 \Omega$ ). Since this type of line imbalance (with  $Z_1 \neq Z_0$ ) is not the usual one in actual differential-mode transmission-line interconnects, the design of the whole structure has not been subjected to the typical requirement of parallel and closely spaced lines. This eases the design and implementation as far as the resistive load necessary for signal balancing ( $Z_\rho = Z_0/\sqrt{2}$ , see previous subsection) is implemented by means of a matched ( $Z_0$ ) termination and a quarter-wavelength impedance inverter. The required impedance of the inverter is simply  $Z_{inv} = Z_0/\sqrt{2} = 42.045 \Omega$ . The considered substrate is *Rogers RO4003C* with dielectric constant  $\epsilon_r = 3.55$ , thickness  $h = 0.8128$  mm, and dissipation factor  $\tan\delta = 0.0022$ , and the operating frequency has been set to  $f_0 = 2.02$  GHz. The simulated electromagnetic response of the structure for frequencies in the vicinity of  $f_0$  is depicted in Fig. 9. From this response, it can be concluded that the output signals have the same modulus and  $180^\circ$  phase balance at  $f_0$ , which means that perfect balance (i.e., a pure differential signal at the output composite port) at that frequency is achieved.

The structure has been fabricated by means of a milling machine *LPKF H100*. The measured response is also included in Fig. 9, where reasonable agreement with the simulated response can be appreciated (taking into account the presence of the *SMD* matched load soldered at the extreme of the stub). Very good signal balancing at  $f_0$  is obtained, as it can be appreciated in Figs. 9(b) and (c).

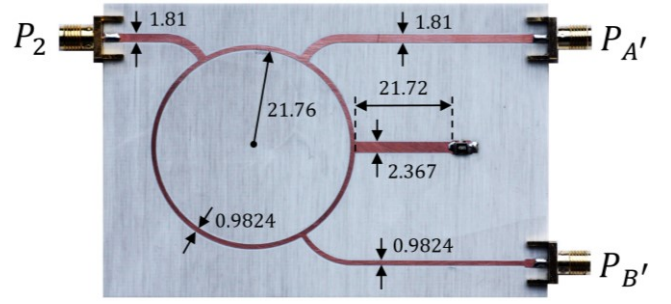


Fig. 8. Photograph of the balancing structure for lines with identical phases and different characteristic impedance. Inset dimensions are given in millimeters). The length of the  $200^\circ$  lines is 49.86 mm, as obtained from the line calculator of *Keysight ADS*.

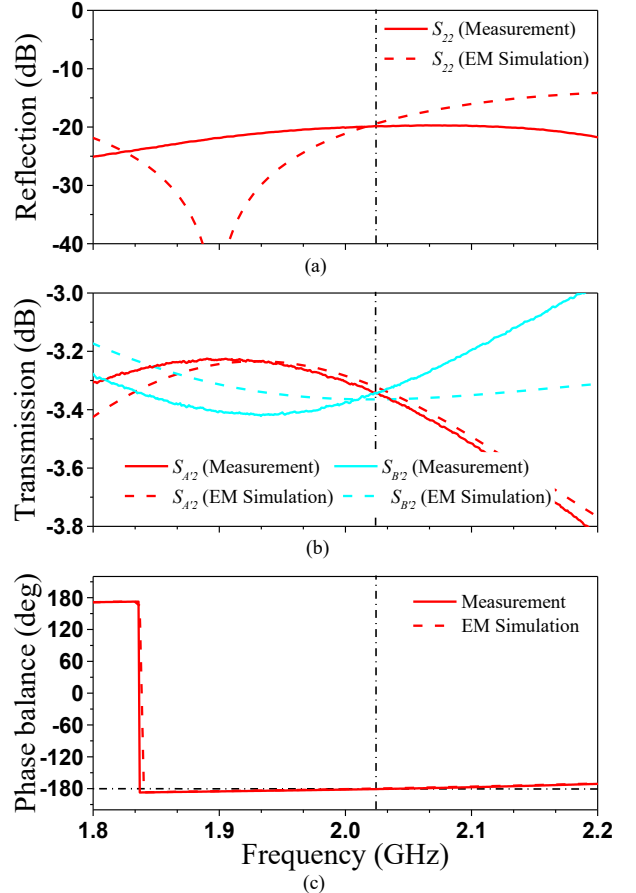


Fig. 9. Frequency response of the structure of Fig. 8. (a) Modulus of  $S_{22}$ , (b) modulus of  $S_{A2}$  and  $S_{B2}$ , and (c) phase balance at the output ports.

For the second case example (line phases set to  $\phi_A = 450^\circ$  and  $\phi_B = 480^\circ$ ), we have generated the layout, and from it we have fabricated the structure (Fig. 10). Among the two possible solutions for the characteristic impedance of line B, we have considered the one corresponding to  $Z_{1,l} = 28.86 \Omega$ , providing a reactive termination of port 1 of the coupler that can be implemented by means of a  $50 \Omega$  open-ended stub with an electrical length of  $135^\circ$ . The simulated and measured frequency responses in the vicinity of  $f_0$  can be seen in Fig. 11. Good agreement between both responses (simulated and measured), as well as signal balancing at  $f_0$ , can be appreciated. Note that in this case line imbalance has been generated by line bending (emulating potential imbalance in a real scenario). With the results of Fig. 11, signal balancing in unbalanced (bended) line pairs is experimentally demonstrated, thereby validating the proposed balancing approach.



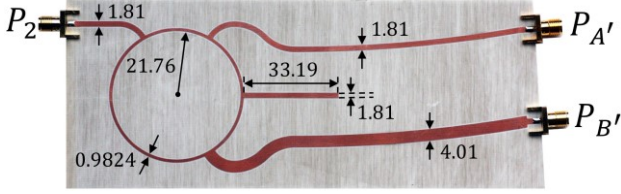


Fig. 10. Photograph of the balancing structure for bended line pairs with unequal electrical length. Inset dimensions are given in mm (millimeters). The length of the 450° and 480° lines is 112.14 mm and 116.57 mm, respectively, as obtained from the line calculator of *Keysight ADS*.

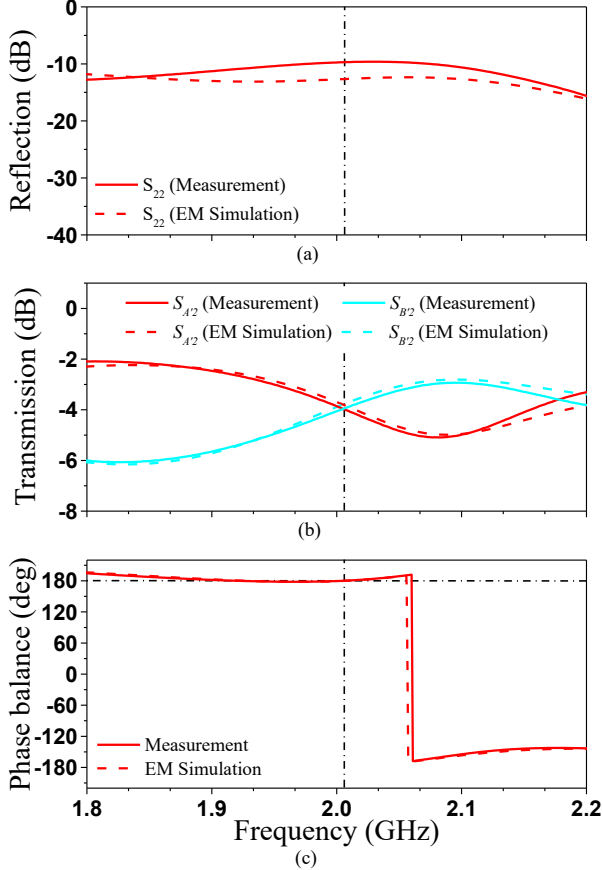


Fig. 11. Frequency response of the structure of Fig. 10. (a) Modulus of  $S_{22}$ , (b) Modulus of  $S_{A'2}$  and  $S_{B'2}$ , and (c) phase balance at the output ports.

## V. DISCUSSION

It is important to mention that signal balancing in unbalanced uncoupled lines by means of a pure reactive load is achieved at the expense of certain level of signal reflection back to the source. This return loss is unavoidable to the light of the reflection coefficient of the structure (expression 12). For the case under study, the reflection coefficient can be written as

$$S_{22} = -\frac{S_{BB}}{2+S_{BB}\rho} \quad (31)$$

and it follows that  $S_{22} \neq 0$  since  $S_{BB} \neq 0$ , as required for signal balancing (see Section III). Introducing  $\rho$  (given by expression 27) and  $S_{BB}$  (expression 15c) in (31), and using (26), the input reflection coefficient is found to be

$$S_{22} = \mp \frac{\cos \phi_A - \cos \phi_B}{2 - \cos \phi_A (\cos \phi_A + \cos \phi_B) - j \sin \phi_A (\cos \phi_A + \cos \phi_B)} \quad (32)$$

Note that (31), and hence (32), verify that  $|S_{22}| \leq 1$ , as required (this can be simply demonstrated from the fact that  $|S_{BB}| \leq 1$  and the modulus of the denominator of expression 31 is larger or equal to one). The fraction of the incident

energy that is reflected back to the source is given by  $|S_{22}|^2$ , which is represented in Fig. 12 for different phase combinations. As the phase difference of both lines decreases, the power reflected back to the source decreases as well. This is an expected result since for  $\phi_A = \phi_B$ , it follows that  $Z_1 = Z_0$  (expression 25), the lines are balanced, and the input signal is totally transmitted to the output ports (out of phase) without reflection, regardless of the termination at port 1 of the coupler, as it is well known.

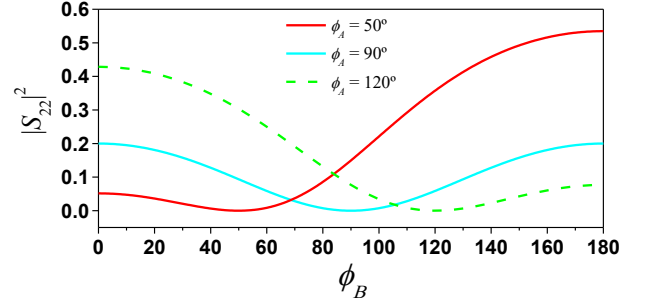


Fig. 12. Fraction of the incident energy reflected back to the source, given by  $|S_{22}|^2$ , as a function of the electrical length of the line B for different electrical lengths of the line A.

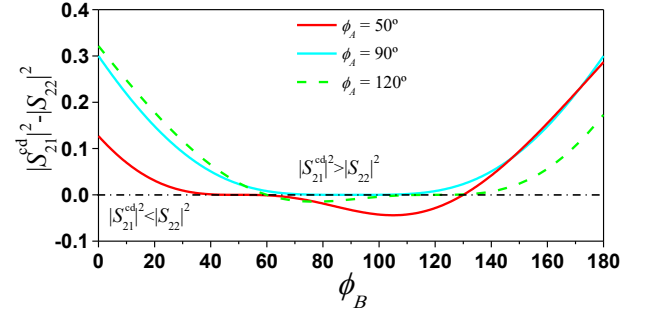


Fig. 13. Loss level comparison between the reported balancing approach (through return loss) and the direct connection of the pair of unbalanced (matched) lines to the rat-race balun (through mode conversion).

The proposed balancing procedure prevents from the presence of common mode signals at the output composite port of the lines, by reflecting part of the incident energy to the source. By contrast, if the balancing procedure reported in this paper is not applied, i.e., the two uncoupled matched lines with phase imbalance are connected directly to the output ports of the coupler, then  $S_{22} = 0$  since  $S_{AA} = S_{BB} = 0$  (provided both lines are matched to the reference impedance of the ports). However, in this case, part of the incident energy is transferred to the common mode at the output composite port of the line pair (as far as  $\phi_A \neq \phi_B$ ), also representing certain loss for the differential mode. The fraction of the energy transferred to the common mode is determined by the cross-mode transmission coefficient of the uncoupled line pair, given by

$$S_{21}^{cd} = \frac{1}{2}(S_{A'A} - S_{B'B}) = \frac{1}{2}(e^{-j\phi_A} - e^{-j\phi_B}) = \frac{\cos \phi_A - \cos \phi_B}{2} - j \frac{\sin \phi_A - \sin \phi_B}{2} \quad (33)$$

In order to compare the loss level of our balancing approach (in the form of return loss) with the loss related to mode conversion when the approach is not applied, we have represented in Fig. 13  $|S_{21}^{cd}|^2 - |S_{22}|^2$ , for the indicated values of  $\phi_A$ , as a function of  $\phi_B$ . For  $\phi_A = 90^\circ$ , the result is positive regardless of  $\phi_B$ , which means that the fraction of the incident energy transmitted to the differential mode is larger when the reported balancing procedure is applied. For other values of  $\phi_A$ , there are values of  $\phi_B$  where  $|S_{21}^{cd}|^2 - |S_{22}|^2 < 0$ ,

but limited to restrictive regions. It can be seen in Fig. 13 that if  $\phi_B$  is in the vicinity of  $\phi_A$ , the usual situation in a practical application, then  $|S_{21}^{\text{cd}}|^2 - |S_{22}|^2 \approx 0$ , which means that the fraction of the incident energy transmitted to the differential mode is comparable in the two considered cases (applying the proposed balancing strategy or not). Nevertheless, in the regions where  $|S_{21}^{\text{cd}}|^2 - |S_{22}|^2 < 0$ , the absolute value is small, and for most values of  $\phi_B$ , it follows that  $|S_{21}^{\text{cd}}|^2 - |S_{22}|^2 > 0$ , resulting in stronger mode conversion loss, as compared to return loss. In summary, not only the common mode at the output composite port of the unbalanced line pair is eliminated with the proposed approach, but also the power associated to the differential-mode signal at that port is, in most cases, higher (as compared to the case where the proposed strategy is ignored, thereby generating mode conversion).

It is clear, according to the previous words, that the reported method for common-mode suppression in the output composite port is not based on the use of common-mode filters. The method is useful to generate a differential-mode signal, with common-mode suppression, from a single-ended signal, by means of a rat-race coupler with a specific termination in the isolated port (as discussed). Thus, the method is of special interest in scenarios involving moderate and narrow band signals.

Comparison to traditional common-mode suppression approaches based on the use of common-mode filters does not provide an advantage to the reported approach in terms of bandwidth. Nevertheless, we have estimated the fractional bandwidth for the structure of Fig. 10, from the experimental results shown in Fig. 11. Note that a pure differential signal at the output port is achieved at the design frequency, where the phase balance is  $180^\circ$  and the modulus of the power splitting transmission coefficients are identical, i.e.,  $S_{A'2} = -S_{B'2}$ . The bandwidth for phase balance has been estimated by considering deviations of  $\pm 5^\circ$  from the nominal value. The resulting phase balance fractional bandwidth has been found to be 10.52 %. Figure 14 depicts both  $(S_{A'2} - S_{B'2})/2$  and  $(S_{A'2} + S_{B'2})/2$ , which are the key parameters providing the equivalent to the differential- and common- mode responses, respectively, of the structure. Note that the whole structure is not a balanced four-port network, but a single-ended to differential-mode converter. It can be appreciated that bandwidth is limited by the common-mode response (see Fig. 14). By considering a common-mode rejection level of 20 dB, the fractional bandwidth is found to be 7.16 %. Nevertheless, the magnitude of the differential-mode response is preserved in the considered frequency range, as far as soft variations in the vicinity of  $-4$  dB can be appreciated. The fractional bandwidth of the input reflection coefficient,  $S_{22}$  [Fig. 11(a)], considering variations of less than 3 dB with regard to the measured value at  $f_0$ , is 17.1%.

In [22], various common-mode filters are compared in terms of common-mode suppression bandwidth and rejection level. As mentioned, the reported single-ended to differential-mode converter device is not as efficient in suppressing the common-mode over a wide band as the common-mode suppression filters reported in [22] and references therein. However, the achieved common-mode rejection ratio (CMRR) at the operating frequency is  $\text{CMRR} = 60.8$  dB, i.e., higher than the CMRR of most devices reported in [22].

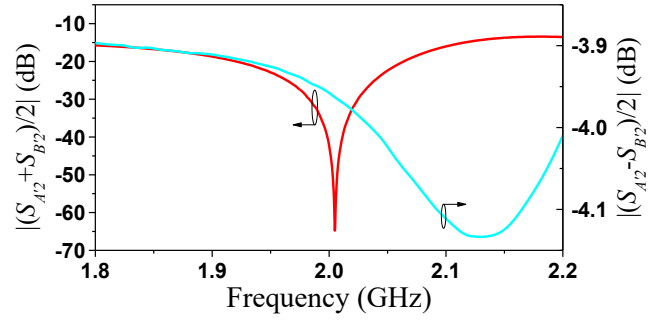


Fig. 14. Representation of  $(S_{A'2} - S_{B'2})/2$  (a) and  $(S_{A'2} + S_{B'2})/2$  (b) for the structure of Fig. 10.

## VI. CONCLUSIONS

In conclusion, it has been demonstrated that a rat-race balun with the isolated port conveniently terminated may be useful to generate balanced (i.e., pure differential-mode) signals at the output composite port of arbitrary (i.e., potentially unbalanced) four port networks. The analysis of the structure has provided us the balance condition, that is, the reflection coefficient of the isolated port of the rat race coupler, necessary to achieve signal balancing. Such reflection coefficient has been expressed in terms of the mixed mode S-parameters of the four-port network, and it is the key design parameter, which in turn determines the necessary load of the isolated port of the rat race. The general analysis has been then applied to the particular case of a pair of uncoupled and unbalanced lines, of interest as far as line bends (unavoidable in many situations) generate phase imbalances in differential line pairs. From such analysis, it has been concluded that signal balancing is only possible by modifying the characteristic impedance of one of the lines; otherwise, the reflection coefficient (the design variable) does not have a finite solution. It has been also demonstrated that with the adequate choice of the impedance of such line (the second design variable), signal balancing is achieved by terminating the isolated port of the rat race coupler with a pure reactance, implementable with an open or short-ended stub. Analytical expressions providing both the characteristic impedance of the line, as well as the reactive impedance of the port termination, as a function of the phases of both lines, have been derived. Finally, the reported balancing approach has been validated through circuit, electromagnetic simulations, and experimental results, by considering unbalanced lines with both phase imbalance (the case of actual interest) and impedance imbalance. The reported balancing approach for bended line pairs (i.e., with phase imbalance), not only suppresses the common mode at the output composite port of the line pair. It also represents an efficient solution in terms of power loss in most cases. The reason is that the return loss, unavoidable in the reported approach and related to the fraction of the incident energy reflected back to the source, in most cases (combinations of line phases) exhibits levels smaller than the loss associated to mode conversion in the bended line pair with matched lines. This means that the energy transfer from the single-ended signal (injected to the input port of the rat-race balun) to the differential-mode signal collected at the output composite port of the bended line pair is, in general (but not in all the cases), more efficient if the reported balancing approach is considered.

## REFERENCES

- [1] W.R. Eisenstadt, B. Stengel, and B.M. Thompson, *Microwave differential circuit design using mixed-mode S-parameters*, Artech House, Norwood, MA, 2006.
- [2] W. Feng, W. Che, and Q. Xue, "The proper balance: overview of microstrip wideband balance circuits with wideband common mode suppression", *IEEE Microw. Mag.*, vol. 16, pp. 55-68, Jun. 2015.
- [3] F. Martín, L. Zhu, J. Hong, and F. Medina, *Balanced Microwave Filters*, Wiley-IEEE Press, Hoboken, NJ, 2018.
- [4] B. C. Tseng and L. K. Wu, "Design of miniaturized common-mode filter by multilayer low-temperature co-fired ceramic", *IEEE Trans. Electromagn. Compat.*, vol. 46, no. 4, pp. 571-579, Nov. 2004.
- [5] W. T. Liu, C.-H. Tsai, T.-W. Han and T.-L. Wu, "An embedded common-mode suppression filter for GHz differential signals using periodic defected ground plane," *IEEE Microw. Wireless Compon. Lett.*, vol. 18, no. 4, pp. 248-250, Apr. 2008.
- [6] S. J. Wu, C. H. Tsai, T. L. Wu, and T. Itoh, "A novel wideband common-mode suppression filter for gigahertz differential signals using coupled patterned ground structure", *IEEE Trans. Microw. Theory Techn.*, vol. 57, no. 4, pp. 848-855, Apr. 2009.
- [7] C.H. Tsai and T.L. Wu, "A broadband and miniaturized common-mode filter for gigahertz differential signals based on negative permittivity metamaterials", *IEEE Trans. Microw. Theory. Techn.*, vol. 58, pp. 195-202, Jan. 2010.
- [8] F. de Paulis, L. Raimondo, Sam Connor, B. Archambeault and A. Orlandi, "Design of a common mode filter by using planar electromagnetic bandgap structures", *IEEE Trans. Adv. Packag.*, vol. 33, no. 4, pp. 994-1002, Nov. 2010.
- [9] J. Naqui *et al.*, "Split rings-based differential transmission lines with common-mode suppression", *IEEE MTT-S Int. Microwave Symposium*, Baltimore (USA), Jun. 2011.
- [10] J. Naqui *et al.*, "Common mode suppression in microstrip differential lines by means of complementary split ring resonators: theory and applications", *IEEE Trans. Microw. Theory Techn.*, vol. 60, pp. 3023-3034, Oct. 2012.
- [11] A. Fernandez-Prieto *et al.*, "Dual-band differential filter using broadband common-mode rejection artificial transmission line", *Prog. Electromagn. Research (PIER)*, vol. 139, pp. 779-797, 2013.
- [12] F.X. Yang, M. Tang, L.S. Wu, and J.F. Mao, "A novel wideband common-mode suppression filter for differential signal transmission", *2014 IEEE Electrical Design of Advanced Packaging & Systems Symposium (EDAPS)*, Bangalore, Dec. 2014, pp. 129-132.
- [13] T.W. Weng, C.H. Tsai, C.H. Chen, D.H. Han and T.L. Wu, "Synthesis model and design of a common-mode bandstop filter (CM-BSF) with an all-pass characteristic for high-speed differential signals", *IEEE Trans. Microw. Theory Techn.*, vol. 62, no. 8, pp. 1647-1656, Aug. 2014.
- [14] G.H. Shiue, C.M. Hsu, C.L. Yeh and C.F. Hsu, "A comprehensive investigation of a common-mode filter for gigahertz differential signals using quarter-wavelength resonators", *IEEE Trans. Compon. Packag., Manuf. Technol.*, vol. 4, no. 1, pp. 134-144, Jan. 2014.
- [15] J. H. Choi, P. W. C. Hon and T. Itoh, "Dispersion analysis and design of planar electromagnetic bandgap ground plane for broadband common-mode suppression", *IEEE Microw. Wireless Comp. Lett.*, vol. 24, no. 11, pp. 772-774, Nov. 2014.
- [16] C.Y. Hsiao, Y.C. Huang, and T.L. Wu, "An ultra-compact common-mode bandstop filter with modified-T circuits in integrated passive device (IPD) process", *IEEE Trans. Microw. Theory Techn.*, vol. 63, no 11, pp. 3624-3631, Nov. 2015.
- [17] A. Fernández-Prieto *et al.*, "Common-mode suppression for balanced bandpass filters in multilayer liquid crystal polymer technology", *IET Microw. Ant. Propag.*, vol. 9, pp. 1249-1253, Sep. 2015.
- [18] B.-F. Su and T.-G. Ma, "Miniaturized common-mode filter using coupled synthetized lines and mushroom resonators for high-speed differential signals", *IEEE Microw. Wireless Compon. Lett.*, vol. 25, pp.112-114, Feb. 2015.
- [19] Z. Zeng, Y. Yao, and Y. Zhuang, "A wideband common-mode suppression filter with compact-defected ground structure pattern", *IEEE Trans. Electromagn. Compt.*, vol. 57, pp. 1277-1280, Oct. 2015.
- [20] P. Vélez, J. Bonache, and F. Martín, "Differential Microstrip Lines with Common-Mode Suppression based on Electromagnetic Bandgaps (EBGs)", *IEEE Ant. Wireless Propag. Lett.*, vol. 14, pp. 40-43, 2015.
- [21] P. Vélez *et al.*, "Enhancing common-mode suppression in microstrip differential lines by means of chirped electromagnetic bandgaps (EBGs)", *Microw. Opt. Technol. Lett.*, vol. 58, pp. 328-332, Feb. 2016.
- [22] F. Martín *et al.*, "The Beauty of Symmetry: Common-Mode Rejection Filters for High-Speed Interconnects and Band Microwave Circuits", *IEEE Microw. Mag.*, vol. 18, no. 1, pp. 42-55, Jan. 2017.
- [23] D.M. Pozar, *Microwave Engineering*, 4<sup>th</sup> Ed., John Wiley, Hoboken, NJ, 2011.
- [24] D.E. Bockelman and W. R. Eisenstadt, "Combined differential and common-mode scattering parameters: theory and simulation", *IEEE Trans. Microw. Theory, Techn.*, vol. 43, pp. 1530-1539, Jul. 1995.
- [25] A. Ferrero and M. Pirola, "Generalized mixed-mode S parameters", *IEEE Trans. Microw. Theory. Techn.*, vol. 54, pp. 458-463, Jan. 2006.



Jonathan Muñoz-Enano was born in Mollet del Vallès (Barcelona), Spain, in 1994. He received the Bachelor's Degree in Electronic Telecommunications Engineering in 2016 and the Master's Degree in Telecommunications Engineering in 2018, both at the Autonomous University of Barcelona (UAB). Actually, he is working in the same university in the elaboration of his PhD, which is focused on the development of microwave sensors based on metamaterials concepts for the dielectric characterization of materials and biosensors.



Paris Vélez (S'10-M'14) was born in Barcelona, Spain, in 1982. He received the degree in Telecommunications Engineering, specializing in electronics, the Electronics Engineering degree, and the Ph.D. degree in Electrical Engineering from the Universitat Autònoma de Barcelona, Barcelona, in 2008, 2010, and 2014, respectively. His Ph.D. thesis concerned common mode suppression differential microwave circuits based on metamaterial concepts and semi-lumped resonators. During the Ph.D., he was awarded with a pre-doctoral teaching and research fellowship by the Spanish Government from 2011 to 2014. From 2015-2017, he was involved in the subjects related to metamaterials sensors for fluidics detection and characterization at LAAS-CNRS through a TECNIOSpring fellowship cofounded by the Marie Curie program. His current research interests include the miniaturization of passive circuits RF/microwave and sensors-based metamaterials through Juan de la Cierva fellowship. Dr. Vélez is a Reviewer for the IEEE Transactions on Microwave Theory and Techniques and for other journals.



Ferran Martín (M'04-SM'08-F'12) was born in Barakaldo (Vizcaya), Spain in 1965. He received the B.S. Degree in Physics from the Universitat Autònoma de Barcelona (UAB) in 1988 and the PhD degree in 1992. From 1994 up to 2006 he was Associate Professor in Electronics at the Departament d'Enginyeria Electrònica (Universitat Autònoma de Barcelona), and since 2007 he is Full Professor of Electronics. In recent years, he has been involved in different research activities including modelling and simulation of electron devices for high frequency applications, millimeter wave and THz generation systems, and the application of electromagnetic bandgaps to microwave and millimeter wave circuits. He is now very active in the field of metamaterials and their application to the miniaturization and optimization of microwave circuits and antennas. Other topics of interest include microwave sensors and RFID systems, with special emphasis on the development of high data capacity chipless-RFID tags. He is the head of the Microwave Engineering, Metamaterials and Antennas Group (GEMMA Group) at UAB, and director of CIMITEC, a research Center on Metamaterials supported by TECNIO (Generalitat de Catalunya). He has organized several international events related to metamaterials and related topics, including Workshops at the IEEE International Microwave Symposium (years 2005 and 2007) and European Microwave Conference (2009, 2015 and 2017), and the Fifth International Congress on Advanced Electromagnetic Materials in Microwaves and Optics (Metamaterials 2011), where he has acted as chair of the Local Organizing Committee. He has acted as Guest Editor for five Special Issues on Metamaterials and Sensors in five International Journals. He has authored and co-authored over 550 technical conference, letter, journal papers and book chapters, he is co-author of the book on Metamaterials entitled *Metamaterials with Negative Parameters: Theory, Design and Microwave Applications* (John Wiley & Sons Inc.), author of the book *Artificial Transmission Lines for RF and Microwave Applications* (John Wiley & Sons Inc.), and co-editor of the book *Balanced Microwave Filters* (John Wiley & Sons Inc.). Ferran Martín has generated

19 PhDs, has filed several patents on metamaterials and has headed several Development Contracts.

Prof. Martín is a member of the IEEE Microwave Theory and Techniques Society (IEEE MTT-S). He is reviewer of the IEEE Transactions on Microwave Theory and Techniques and IEEE Microwave and Wireless Components Letters, among many other journals, and he serves as member of the Editorial Board of IET Microwaves, Antennas and Propagation, International Journal of RF and Microwave Computer-Aided Engineering, and Sensors. He is also a member of the Technical Committees of the European Microwave Conference (EuMC) and International Congress on Advanced Electromagnetic Materials in Microwaves and Optics (Metamaterials). Among his distinctions, Ferran Martín has received the 2006 Duran Farell Prize for Technological Research, he holds the *Parc de Recerca UAB – Santander* Technology Transfer Chair, and he has been the recipient of three ICREA ACADEMIA Awards (calls 2008, 2013 and 2018). He is Fellow of the IEEE and IET.